Chinese Medical Journal®

Promotion effect of FOXCUT as a microRNA sponge for miR-24-3p on progression in triple-negative breast cancer through the p38 MAPK signaling pathway

Xiafei Yu, Fangze Qian, Xiaoqiang Zhang, Yanhui Zhu, Gao He, Junzhe Yang, Xian Wu, Yi Zhou, Li Shen, Xiaoyue Shi, Hongfei Zhang, Xiao'an Liu

Department of Breast Surgery, The First Affiliated Hospital of Nanjing Medical University, Nanjing, Jiangsu 210029, China.

Abstract

Background: Triple-negative breast cancer (TNBC) is a type of highly invasive breast cancer with a poor prognosis. According to new research, long noncoding RNAs (lncRNAs) play a significant role in the progression of cancer. Although the role of lncRNAs in breast cancer has been well reported, few studies have focused on TNBC. This study aimed to explore the biological function and clinical significance of forkhead box C1 promoter upstream transcript (FOXCUT) in triple-negative breast cancer.

Methods: Based on a bioinformatic analysis of the cancer genome atlas (TCGA) database, we detected that the lncRNA FOXCUT was overexpressed in TNBC tissues, which was further validated in an external cohort of tissues from the General Surgery Department of the First Affiliated Hospital of Nanjing Medical University. The functions of FOXCUT in proliferation, migration, and invasion were detected *in vitro* or *in vivo*. Luciferase assays and RNA immunoprecipitation (RIP) were performed to reveal that FOXCUT acted as a competitive endogenous RNA (ceRNA) for the microRNA miR-24-3p and consequently inhibited the degradation of p38.

Results: lncRNA FOXCUT was markedly highly expressed in breast cancer, which was associated with poor prognosis in some cases. Knockdown of FOXCUT significantly inhibited cancer growth and metastasis *in vitro* or *in vivo*. Mechanistically, FOXCUT competitively bounded to miR-24-3p to prevent the degradation of p38, which might act as an oncogene in breast cancer.

Conclusion: Collectively, this research revealed a novel FOXCUT/miR-24-3p/p38 axis that affected breast cancer progression and suggested that the lncRNA FOXCUT could be a diagnostic marker and therapeutic target for breast cancer.

Keywords: Triple negative breast neoplasms; RNA, long noncoding; FOXCUT; miR-24-3p; p38 MAPK signaling pathway; Disease progression

Introduction

According to the latest epidemiological data, breast cancer (BC) has become the most prevalent cancer, and is expected to account for 12.9% of new cancer cases in 2023.[1] Although the long-term survival rate of early BC is better than that in other cancer types, some patients still develop local and distant recurrence in a short period of time.[2] There are five major subtypes of tumor heterogeneity in BC, and the treatment programs and clinical treatment effect are different among these BC subtypes. Therefore, it is important to elucidate the molecular mechanism and development of BC.[3]

Triple-negative breast cancer (TNBC) is the most aggressive BC subtype, with poor survival rates,[4] onset at a younger age, and a proclivity for distant metastasis.[5] Furthermore, it is a heterogeneous disease with a complex genetic background,[6] and thus patients exhibit variable prognoses and responses to chemotherapies.[7,8] Decades of research on TNBC have yielded numerous results, and many new treatment options have been developed over the past few years, such as antibody-drug conjugates (ADCs), immune-checkpoint inhibitors (ICIs), PARP inhibitors, and other agents and combinations.[5] However, current treatment outcomes are unsatisfactory even with targeted therapy and immunotherapy, so unfortunately, chemotherapy remains the preferred treatment.[9] As a result, finding new targets and understanding their mechanisms is critical.

In recent years, whole genomic and transcriptomic studies have indicated that the genome of *Homo sapiens*

Access this article online

Quick Response Code:

Website: www.cmj.org

DOI: 10.1097/CM9.0000000000002700

Correspondence to: Xiao'an Liu, Department of Breast Surgery, The First Affiliated Hospital of Nanjing Medical University, Nanjing, Jiangsu 210029, China
E-Mail: liuxiaoan@126.com

Chinese Medical Journal 2024;137(1)

Received: 12-12-2022; **Online:** 20-07-2023 **Edited by:** Xiuyuan Hao

encodes many noncoding RNAs. Long-chain noncoding RNAs (lncRNAs) which do not have the function of coding proteins, are >200 nucleotides in size and lack a complete open reading frame.[10] MicroRNAs (miRNAs) are short RNAs of 19–25 nucleotides that regulate post-transcriptional silencing of target genes. miRNAs have been considered to participate in the pathogenesis of many benign and malignant diseases, including cancer, eosinophilic esophagitis, and cardiovascular and cerebrovascular diseases.[11–13] Increasing evidence suggests that lncRNAs may compete for miRNA binding as competing endogenous RNAs (ceRNAs), influencing various biological functions, such as cellular growth, invasion, and differentiation. For example, a novel lncRNA BCRT1/miR-1303/PTBP3 pathway promoted exosome-mediated M2 macrophage polarization and increased the BC progression rate.[14] H19, another well-known lncRNA, plays a oncogenic role in BC invasion and metastasis by binding with miR-675 at the first intron and suppressing its expression.[15,16]

Forkhead box C1 promoter upstream transcript (FOXCUT) activates the PI3K/AKT pathway and modulates colorectal cancer cell growth and proliferation by regulating FOXC1 and MMP1 expression. Studies have shown that *FOXCUT* is located on chromosome 6p25.3 and plays an important regulatory role in several diseases, such as colon and gastric cancer.[17,18] Wang *et al*[19] found that miR-296-3p and FOXCUT acted as tumor-suppressing factors and upregulated MMP2/MMP9, thus promoting angiogenesis and tumor metastasis in choroidal malignant melanoma. In this work, we aimed to explore the biological function and clinical significance of FOXCUT in triple-negative breast cancer. Thus, our findings provided new insights into the molecular mechanisms and diagnostic and prognostic markers of BC.

Methods

Ethical approval

This research was approved by the Ethics Committee of the First Affiliated Hospital of Nanjing Medical University (No. 2021SR184). All patients signed informed consent before tissue specimen collection.

Tissue samples

A total of 224 pairs of breast tumor tissues and corresponding paracancerous tissues were collected from the General Surgery Department of the First Affiliated Hospital of Nanjing Medical University between 2016 and 2018. 196 pairs of these tissues were subjected to human RNA sequence (RNA-seq), and the remaining 28 pairs of tissues were mainly used for quantitative real-time polymerase chain reaction (qRT-PCR) verification. All collected samples were immediately snap frozen and stored in liquid nitrogen until needed.

RNA sequencing analysis

This research was based on RNA sequence data of 196 BC tissues derived from our center. The statistical analysis was performed with GraphPad Prism 6 (version 6.01, GraphPad Software, California, USA) and R programming software (version 4.0, https://www.r-project.org/about.html) using the DESeq2 package (version 2.0, http://www.bioconductor.org/packages/release/bioc/vignettes/Glimma/inst/doc/DESeq2.html). Two-tailed Student's *t* tests and Wilcoxon tests were performed for comparisons. Log_2|fold change| ≥1 and a two-sided *P*-value <0.05 were considered statistically significant.

Cell culture

Seven human BC cell lines, MDA-MB-468, MDA-MB-231, BT-549, T47D, SK-BR-3, ZR75-1, and MCF-7, the normal human breast epithelial cell line MCF-10A and the human embryonic kidney cell line HEK-293T studied in this article were obtained from the Cell Bank of the Chinese Academy of Sciences (Shanghai, China). The aforementioned cells were grown in Dulbecco's modified medium containing 10% fetal bovine serum (Wisent, Montreal, Canada) with 1% Penicillin–Streptomycin (Gibco, Rockville, USA). All cells were incubated in a 37°C humidified incubator containing 5% CO_2.

RNA extraction and qRT-PCR assays

Total RNA was isolated from cells and tissues using TRIzol Reagent (Life, CA, USA), and mRNA expression was detected by qRT-PCR using SYBR green master mix (Vazyme, Nanjing, China). Reverse transcription of miRNA was performed using a One Step PrimeScript miRNA cDNA Synthesis Kit (TaKaRa, Kyoto, Japan). The relative expression of miRNA was normalized to U6 expression levels. The primers used in this research are uploaded in Supplementary Tables 1 and 2, http://links.lww.com/CM9/B556. The analysis of RNA expression was calculated using the $2^{-\Delta\Delta CT}$ method.

Transwell assays

Transwell chambers (pore size 8 μm; Millipore Corporation, Massachusetts, USA) with or without Matrigel (BD Biosciences, New York, USA) were used to perform the transwell assay. A total of 2×10^4 cells were added to the upper insert, and 700 μL of medium with 20% FBS as a chemoattractant was added to the lower surface. Then, the cells that migrated to the lower chamber were fixed with ethanol and stained with 0.2% crystal violet after incubation for 24–48 h, and the cell number was counted.

Western blot assay and antibodies

Total protein from tissues and cell lines was extracted by Radio Immuno Precipitation Assay (RIPA) lysis buffer (Beyotime, Shanghai, China), added to 10% sodium sulfate polyacrylamide gel (SDS-PAGE) and transferred onto 0.22 μm polyvinylidene fluoride (PVDF) membranes (Millipore, Massachusetts, USA). Subsequently, specific antibodies against p38, CDK1, CDK2, CDK4, vimentin, cyclin D1, and GAPDH were used [Supplementary Table 3, http://links.lww.com/CM9/B556]. The membranes

were blocked with 5% skim milk powder and incubated with primary antibodies at 4°C overnight. After that, a chemiluminescence horseradish peroxidase (HRP) Substrate (Millipore, Massachusetts, USA) system was used to visualize the protein blots.

Animal experiments

The animal procedures were approved by the Nanjing Medical University Animal Care and Use Committee (No. 2208012). To test the effects of FOXCUT on tumor growth, a total of 1×10^6 of luciferase-expressing cells with or without FOXCUT overexpression were injected (inoculated) subcutaneously into the fat pads of each flank of 4–6-week-old BALB/c nu/nu female mice twice per day. When a tumor was palpable, a dial caliper was used to measure its longest diameter and widest vertical width every four days. Then, its volume was calculated by the formula ($V = \text{length} \times \text{width}^2 \times 0.5$). At the end of animal experiments, the mice were sacrificed, and the tumors were surgically removed, measured, weighed, and photographed. The mice were euthanized and dissected at the end of the experiment.

TdT-mediated dUTP nick-end labeling (TUNEL) staining assay

Paraffin-embedded tissue sections were stained with the TUNEL Apoptosis Detection Kit (Alexa Fluor 640) (Yeasen, Shanghai, China) according to the manufacturer's protocol. Images were acquired with an Olympus fluorescence microscope (Olympus, Tokyo, Japan).

Fluorescence in situ hybridization (FISH) and subcellular fractionation assay

For FISH, we chose the TNBC cells MDA-MB-231. They were grown on glass coverslips in 24-well plates for one night. Then, the prepared cells were fixed with paraformaldehyde. Next, they were hybridized with Cyanine3 (Cy3)-labeled probes designed and synthesized by GenePharma (Shanghai, China), and the nuclei were stained with 2-(4-Amidinophenyl)-6-indolecarbamidine (DAPI) dihydrochloride (Sigma-Aldrich, Massachusetts, USA). A fluorescence microscope (Nikon, Tokyo, Japan) was then used to observe the staining results. Protein and RNA isolation system (PARIS™) kit (Thermo Fisher Scientific, Massachusetts, USA) was used to isolate nuclear and cytoplasmic fractions. Cells were lysed in cell fraction buffer on ice and subsequently centrifuged at $500 \times g$ for 3 min at 4°C, and the supernatant was collected as the cytoplasmic fraction. The pelleted nuclei were incubated with cell disruption buffer and used as the nuclear fraction. Then, the RNAs of these two fractions were extracted and detected by qRT-PCR.

Dual luciferase reporter assay

The wild-type FOXCUT and p38 reporter vectors were formed by amplifying and cloning segments of FOXCUT or p38 into the pmirGLO vector (Abcam, Boston, US). miR-24-3p-mut was also generated by inserting corresponding mutant FOXCUT fragments into the vectors. Then, 5000 cells per well were seeded in 96-well plates and cotransfected with the miR-24-3p and or control vector by Lipofectamine (Invitrogen, CA, USA) according to the manufacturer's recommendation. Finally, the luciferase activity was detected by employing a Dual-Luciferase Reporter Assay System (Promega, Madison, USA) at 48 h after transfection.

Clonogenic survival assay

For colony formation assays, BC cells were diluted to a concentration of 1000 cells per 200 μL and seeded at a density of 1000 cells per well in 6-well cell culture plates. The cells were then allowed to grow at 37°C in a humidified 5% CO_2 atmosphere. After 14 days, cell colonies were washed with phosphate buffer saline, fixed with methanol, and stained with 0.1% crystal violet (Beyotime, Shanghai, China) according to the manufacturer's instructions. Then, the visible colonies on the plates were imaged and calculated by a gel documentation system (Bio-Rad, Hercules, USA).

Results

Upregulation of FOXCUT was associated with poor prognosis in TNBC

In our study, lncRNAs that could potentially affect BC pathogenesis were identified from The Cancer Genome Atlas (TCGA) dataset. Compared with paracancerous tissue, the lncRNA FOXCUT was highly expressed in BC tissues, especially in TNBC tissue samples [Figure 1A]. Our center used an external validation cohort consisting of 196 tissues from our BC RNA-seq data, the differentially expressed genes between basal like type and normal, HER2+ , luminal A, luminal B types were analyzed and the validation results were consistent with TCGA database analysis [Figure 1B]. Notably, the expression of FOXCUT was higher in basal like tissues [Figure 1C], suggesting that FOXCUT might be related to BC progression. Then, FOXCUT levels in BC cell lines were tested, and the results showed that compared with the MCF-10A cell line, FOXCUT was highly expressed in BC cells [Figure 1D]. We also analyzed the differential expression of FOXCUT among patients from in-house database in the different clinical stage, M stage and N stage [Figure 1E, Supplementary Table 4, http://links.lww.com/CM9/B556]. In general, the above data indicated that FOXCUT was upregulated in TNBC.

Downregulation of FOXCUT attenuated BC cell growth

To study the effect of FOXCUT on BC occurrence, MDA-MB-231 and BT549 cell lines that showed high expression of FOXCUT were transfected with siRNAs against FOXCUT (siRNA1#, 2#; Figure 2A). The growth curves generated from cell count kit-8 (CCK8) assays showed that knockdown of FOXCUT strongly inhibited the growth of BC cells [Figure 2B]. In addition, colony formation analysis showed the same results as the silenced FOXCUT experiment in Figure 2C. To further illustrate the carcinogenic effects of FOXCUT *in vivo*, we subcutaneously injected BC cells transfected with a lentiviral vector containing FOXCUT-targeting

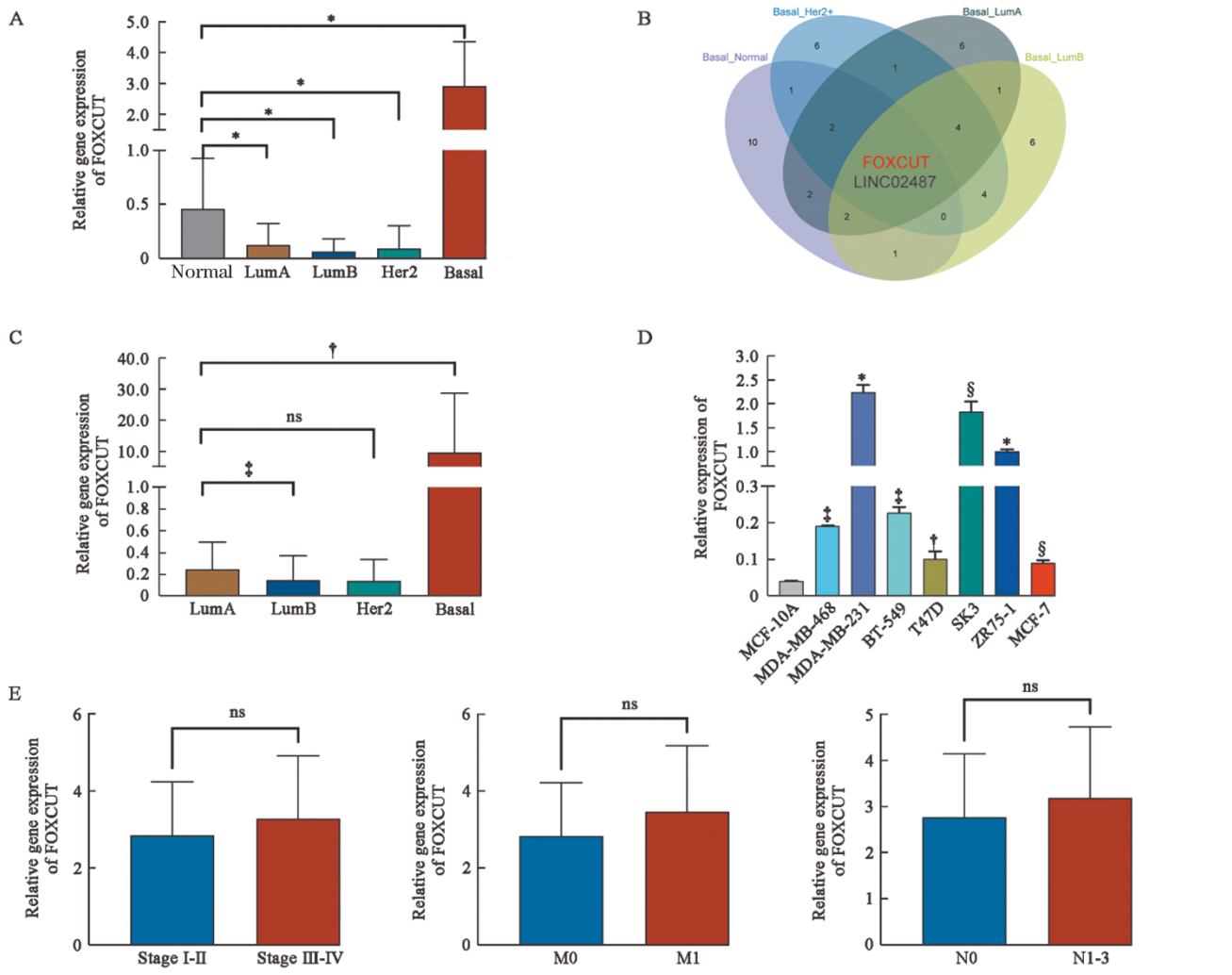

Figure 1: Expression of FOXCUT in breast cancer tissues and cells. (A) Expression of FOXCUT in different samples in TCGA database. (B) Specifically highly expressed lncRNAs (FOXCUT and LINC02487) in basal-like breast cancer tissues. Basal_Normal: differentially expressed genes of basal type *vs.* normal tissue. Basal_Her2+: differentially expressed genes of basal *vs.* Her2+ type. Basal_LumA: differentially expressed genes of basal *vs.* luminal A type. Basal_LumB: differentially expressed genes of basal *vs.* luminal B type. (C) Expression of FOXCUT in different molecular types of breast cancer tissues. (D) Expression of FOXCUT in different breast cancer cell lines. (E) The difference of FOXCUT expression in different clinicopathological group (clinic stage, M stage and N stage). Values are expressed as the means ± standard deviation. $^{*}P$ <0.0001, $^{\dagger}P$ <0.01, $^{\ddagger}P$ <0.05, and $^{\S}P$ <0.001. lncRNA: Long noncoding RNAs; ns: Not significant; TCGA: The cancer genome atlas.

siRNA sequences into the flanks of 4-week-old female athymic BALB/c mice [Figure 2D]. Compared with the control, the tumor formation rate of the FOXCUT knockdown group was significantly reduced, and the tumor growth of the FOXCUT knockdown mice was also considerably slowed [Figure 2E]. Besides, after knockdown of FOXCUT, TUNEL staining of MDA-MB-231 cells showed that the number of apoptotic cells increased [Figure 2F]. Undoubtedly, these data verified the important role of FOXCUT in regulating the proliferation of BC cells.

Knockdown of FOXCUT attenuated cell migration and invasion

In this study, we further elaborated the functional significance of FOXCUT in BC cell migration and invasion. To examine the effect of FOXCUT knockdown on BC cell metastasis, transwell assays were carried out. Notably, the number of cells that passed through the transwell chamber in the FOXCUT knockdown group was less than that in the control group [Figure 2G]. Wound healing assays also showed that the migration of BC cells was impaired by FOXCUT knockdown [Figure 2H].

FOXCUT functioned as a sponge for miR-24-3p in BC cells

According to reports, a large number of lncRNAs act as microRNA sponges to execute their ceRNA functions.[27] Our study found that FOXCUT was mainly located in the cytoplasm of BCs using subcellular fractionation and FISH. This result suggested that FOXCUT might regulate target expression at the posttranscriptional level [Figure 3A,B]. Through the online prediction tools AnnoLnc (http://annolnc.cbi.pku.edu.cn) and LncBook (https://ngdc.cncb.ac.cn/lncbook/), we observed that the sequence of FOXCUT contained an abundance of potential miR-24-3p, miR-9-5p, miR-212-5p, and miR-147b-3p binding sites [Figure 3C]. In addition, BC

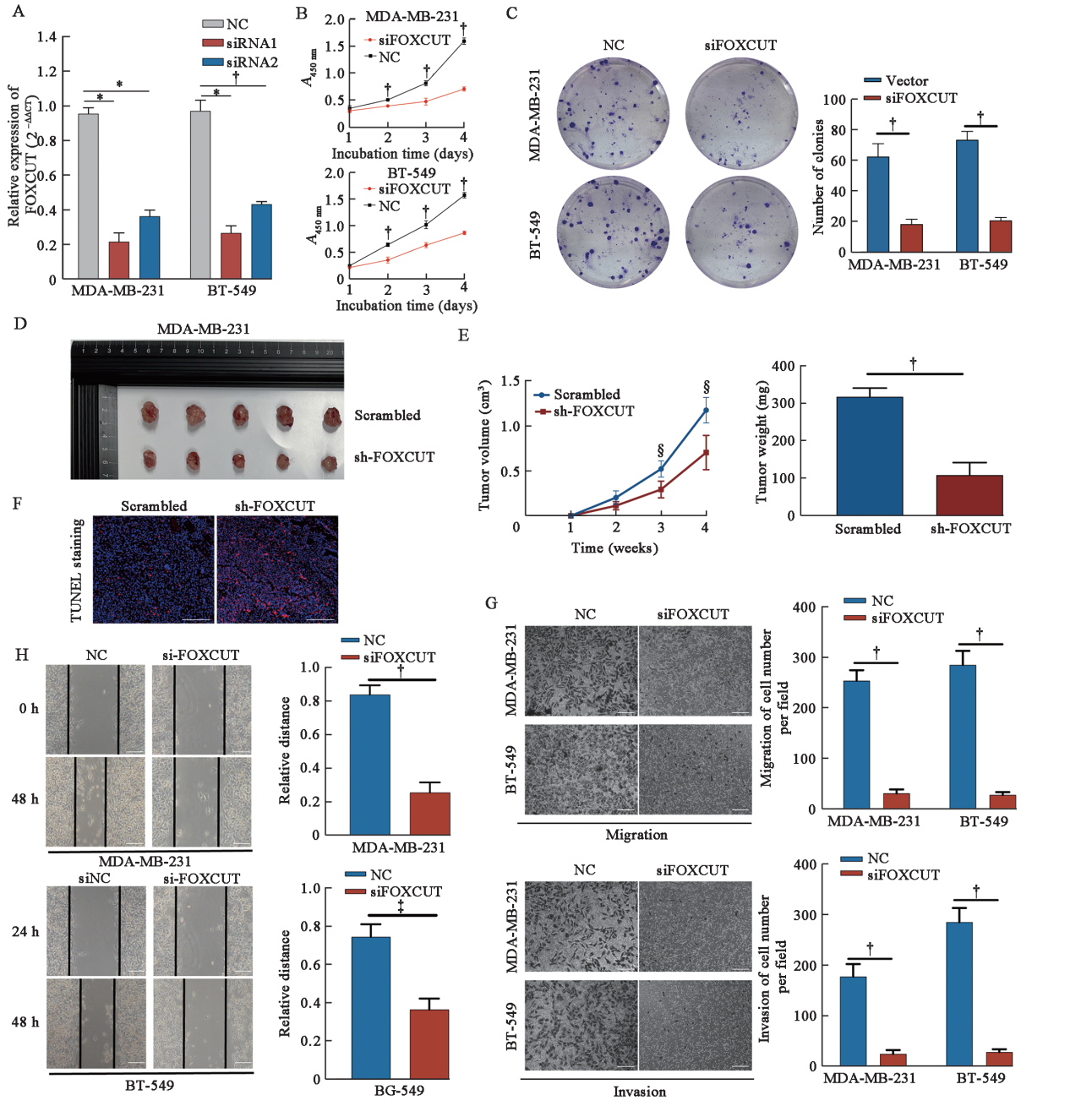

Figure 2: The functional experiment of FOXCUT in breast cancer cell lines. (A,B) Construction of siRNA to knock down FOXCUT expression in triple-negative breast cancer cell lines. The CCK8 assay showed knockdown of FOXCUT expression reduced the proliferation of breast cancer cells. (C) Colony formation assays were performed in breast cancer cells transfected with siFOXCUT siRNAs. (D) Representative picture of subcutaneous xenograft tumors ($n = 5$ for each group). (E) Curves of tumor volumes and weights showed negative effects of FOXUT knockdown on the formation of subcutaneous xenograft tumors. (F) TUNEL staining of MDA-MB-231 cells after knockdown of FOXCUT. Scale bar = 50 μm. (G) The transwell assay showed knockdown of FOXCUT expression reduced the migration and invasion of breast cancer cells. Scale bar = 100 μm. (H) The wound healing assay showed knockdown of FOXCUT expression reduced the migration of breast cancer cells. Scale bar = 100 μm. Values are expressed as the mean ± standard deviation. $^{*}P$ <0.0001, $^{\dagger}P$ <0.001, $^{\ddagger}P$ <0.01. CCK-8: Cell count kit-8.NC: Negative control; ns: Not significant. TUNEL: TdT-mediated dUTP nick-end labeling. siRNA: Small interfering RNA.

cell extracts were subjected to an RNA-binding protein immunoprecipitation (RIP) assay, which showed that FOXCUT directly binded to Ago2, a key component of the miRNA-mediated RNA-induced silencing complex [Figure 3D]. To further validate the predicted results, we performed a dual-luciferase gene reporter assay. Moreover, qRT-PCR analysis revealed that the expression level of miR-24-3p was negatively regulated by FOXCUT. Moreover, miR-24-3p exhibited the most pronounced changes after knockdown of FOXCUT [Figure 3E]. The experimental results showed that only upregulated miR-24-3p and miR-9-5p could decrease FOXCUT-driven luciferase activity, while other miRNAs failed to produce similar effects [Figure 3F]. While miR-9-5p had no significant effect on the migration function of breast cancer cells [Supplementary Figure 1, http://links.lww.com/CM9/B556]. Therefore, we specifically investigated the association between FOXCUT and miR-24-3p. We designed

luciferase reporter genes containing a mutated FOXCUT sequence that altered miR-24-3p potential binding sites, which were then transfected into 293T cells with and without miR-24-3p [Figure 3G]. We observed that the inhibitory effects of miR-24-3p on luciferase activity could be abolished by the mutated FOXCUT sequence [Figure 3H]. Through analysis of 28 TNBC tumor tissue samples, we uncovered a significantly negative correlation between FOXCUT and miR-24-3p ($r = -0.6246$, $P = 0.0004$) [Figure 3I]. Collectively, these results revealed that FOXCUT physically interacted with miR-24-3p and might act as a ceRNA for miR-24-3p. Furthermore, Transwell and CCK8 assays indicated that overexpression of miR-24-3p could partly rescue the tumor-promoting effect of FOXCUT overexpression on BC cells [Figure 4A,B].

LncRNA FOXCUT upregulated p38 expression via inhibition of miR-24-3p

To identify the downstream target genes of miR-24-3p, online tools such as TargetScan (http://www. targetscan. org/vert_71/), miRWalk (http://mirwalk.umm.uni-heidelberg.de/), and miRDB (http://www. mirdb.org/cgi-bin/search.cgi) were searched, followed by analysis of RNA-sequencing data from knockdown FOXCUT in the MDA-MB-231 cell line. Compared with wild-type cells, the differentially expressed

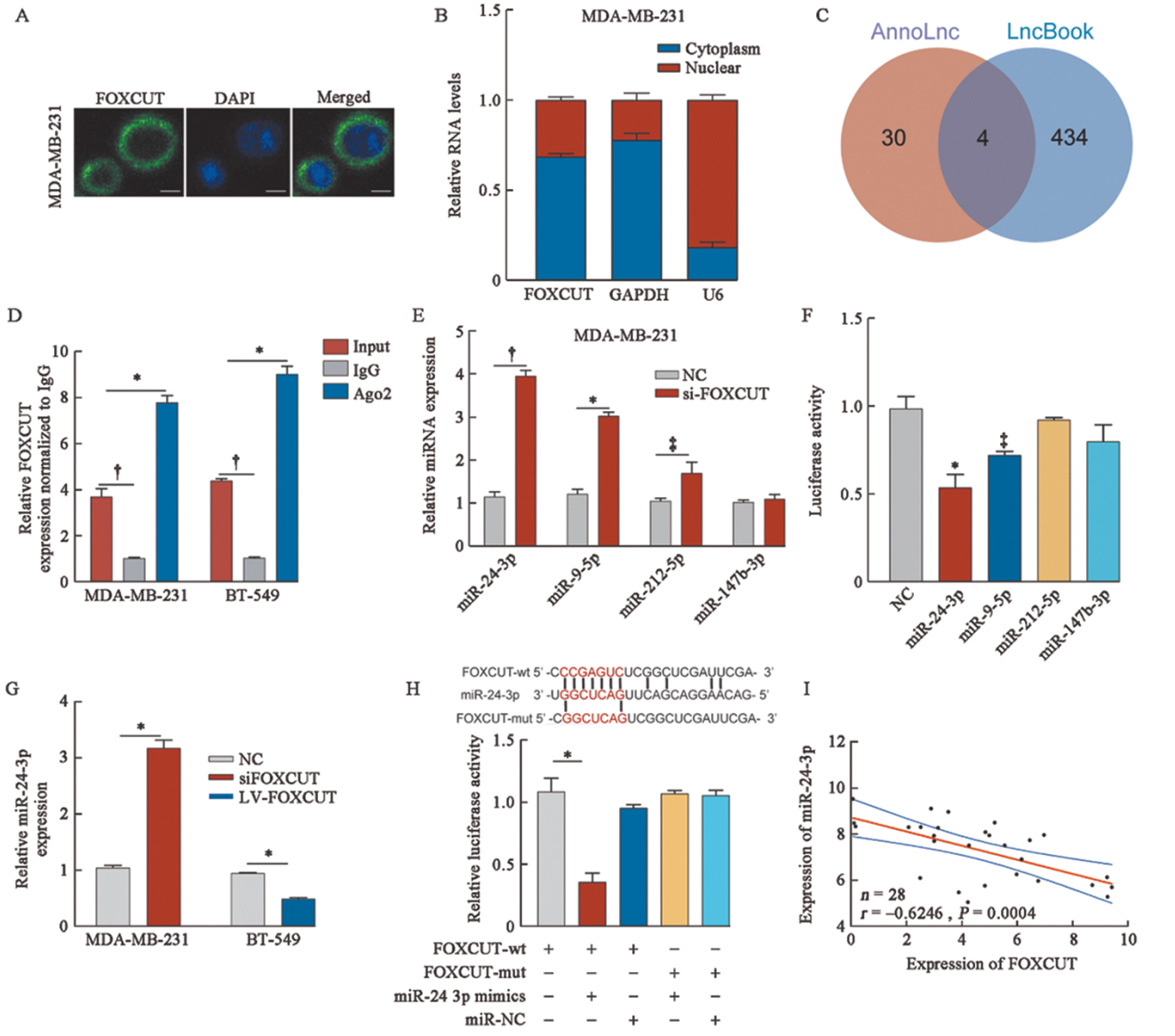

Figure 3: Screening of downstream target genes by RNA sequencing. (A) The subcellular location of FOXCUT in MDA-MB-231 cells was investigated by FISH. Scale bar = 100 μm. (B) Nuclear-cytoplasmic fractionation assay identified the localization of FOXCUT. GAPDH and U6 were used as cytoplasmic and nuclear controls, respectively. (C) Venn diagram showing the overlap of the target miRNAs of FOXCUT predicted by AnnoLnc (http://annolnc.cbi.pku.edu.cn) and LncBook (https://ngdc.cncb.ac.cn/lncbook/). (D) RIP assay to detect downstream miRNA. (E) qRT-PCR analysis revealed that the expression level of miR-24-3p was negatively regulated by FOXCUT. (F) Dual-luciferase reporter gene assay was used to detect the effect of FOXCUT on downstream genes and to screen target genes. (G) The interference effect of FOXCUT on miR-24-3p was verified by qRT-PCR assay, and a schematic of the wild-type (wt) and mutant (mut) FOXCUT luciferase reporter vectors. (H) Luciferase reporter gene assay was used to illustrate the regulatory relationship between FOXCUT and miR-24-3p. (I) Correlation analysis of qRT-PCR data between FOXCUT and miR-24-3p. Values are expressed as the mean ± standard deviation. $^{*}P$ <0.01, $^{\dagger}P$ <0.001 and, $^{\ddagger}P$ <0.05. FISH: Fluorescence *in situ* hybridization. NC: Negative control. qRT-PCR: Quantitative real-time polymerase chain reaction. RIP: RNA immunoprecipitation.

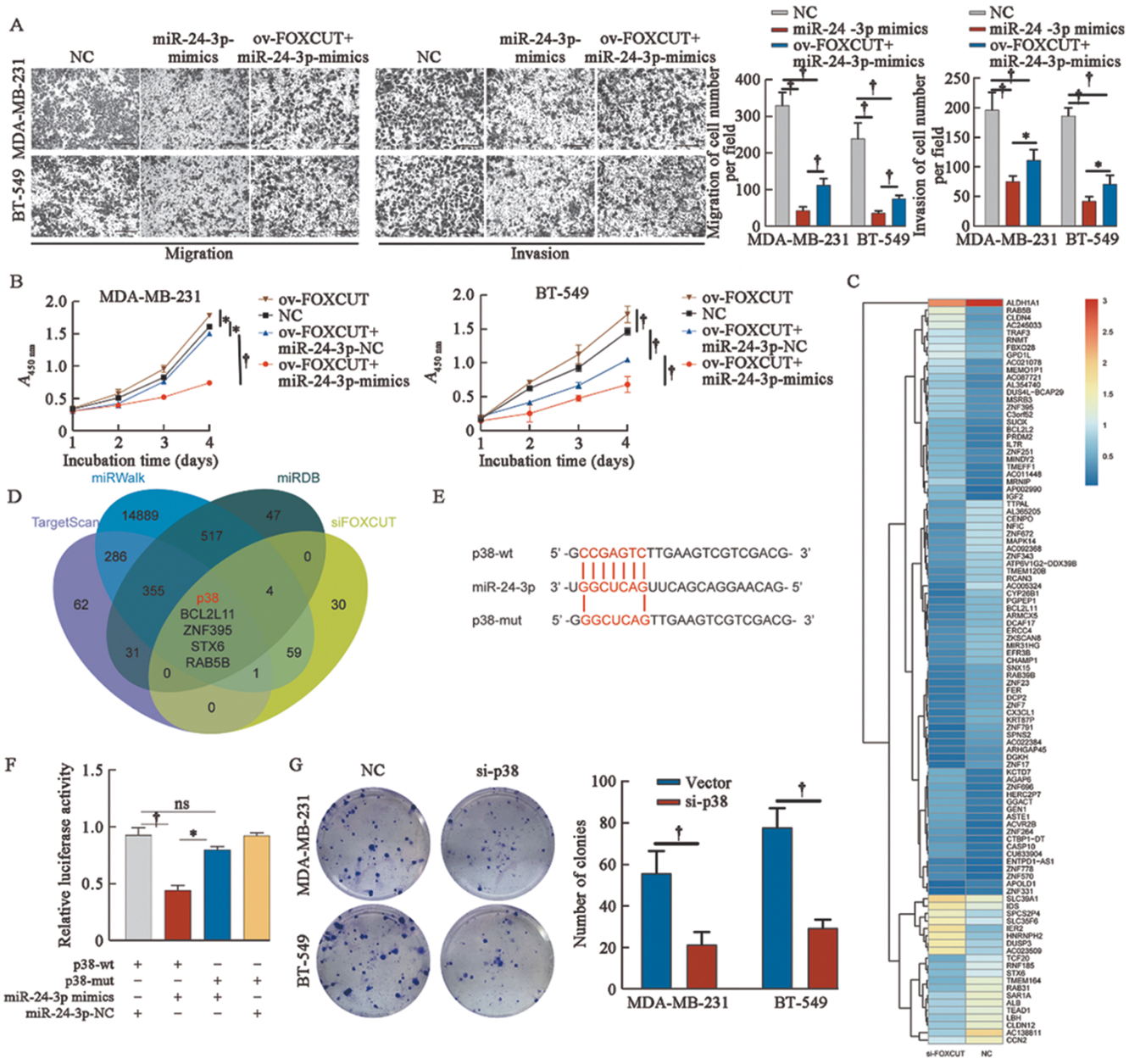

Figure 4: FOXCUT upregulated the downstream target gene *p38* by inhibiting miR-24-3p. (A, B) Migration and invasion assays and CCK8 assays were used to reflect the effects of FOXCUT on downstream miR-24-3p in regulating cell proliferation and migration. Scale bar = 100 mm. (C,D) Bioinformatics prediction via TargetScan, miRWalk, miRDB, and RNA-seq after knockdown of FOXCUT to search the downstream target genes of miR-24-3p comprehensively. (E) A schematic of the wild-type (wt) and mutant (mut) p38 luciferase reporter vectors. (F) Luciferase reporter gene was used to detect the interaction between miR-24-3p and p38. (G) Colony formation assays were used to verify the effects of miR-24-3p and p38 on the function of breast cancer cell lines. Scale bar = 100 μm (original magnification 200 ×). Values are expressed as the mean ± standard deviation. $^{*}P$ <0.01, and $^{\dagger}P$ <0.001. CCK8: Cell count kit-8. NC: Negative control. ns: Not significant. ov: Overexpression.

genes in the FOXCUT knockdown cells are shown in Figure 4C. Finally, *p38*, *BCL2L11*, *ZNF395*, *STX6*, and *RAB5B* were confirmed as candidate genes [Figure 4D]. However, based on the existing research,[40,41] further research led to the choice of p38 as the target. Collectively, we constructed a mutant p38 plasmid according to the ligation site for further study [Figure 4E]. The luciferase assay revealed that upregulating miR-24-3p reduced the luciferase activity of the wild-type p38 reporter but not that of the mutant reporter [Figure 4F], indicating that miR-24-3p could directly target p38. Furthermore, colony formation analysis showed that knockdown of p38 strongly inhibited the growth of BC cells, as displayed in Figure 4G. Moreover, FOXCUT was found to be positively correlated with p38 in 28 pairs of BC and paracancerous tissues (r = 0.6774, P <0.0001) [Figure 5A]. CCK8 and transwell assays showed that knockdown of p38 reduced the proliferation, migration, and invasion of BC cells [Figure 5B,C]. These results suggested that p38 acted as a proto-oncogene in BC and that FOXCUT played an important role in regulating p38 expression through miR-24-3p. Moreover, knockdown of FOXCUT induced apop-

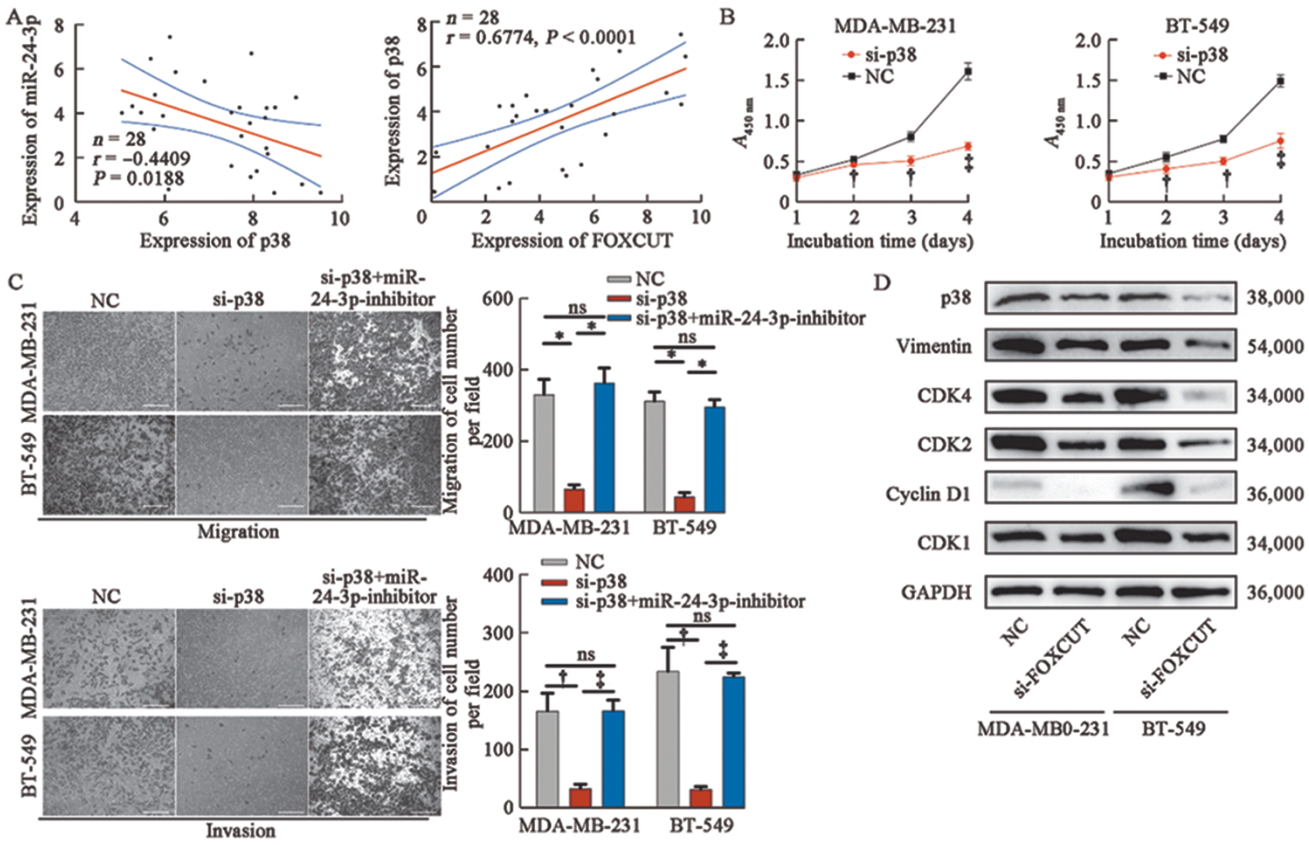

Figure 5: p38 was indirectly regulated by FOXCUT. (A) The correlation between the expression levels of FOXCUT/miR-24-3, and p38 was verified by qRT-PCR in 28 pairs of triple-negative breast cancer tissues. (B,C) Knockdown of p38 expression in breast cancer cell lines reduced cell proliferation and migration ability. (D) Knockdown of FOXCUT expression effected the expression of breast cancer cell cycle-related proteins. Scale bar = 100 μm (original magnification 200 ×). Values are expressed as the mean ± standard deviation. $^{*}P$ <0.0001, $^{\dagger}P$ <0.01, and $^{\ddagger}P$ <0.001. NC: Negative control. ns: Not significant. qRT-PCR: Quantitative real-time polymerase chain reaction.

tosis and reduced S-phase checkpoint proteins such as CDK1 and CDK2 [Figure 5D]. Downregulation of FOXCUT also impaired BC cell invasion and migration.

Discussion

The condition of patients with TNBC is relatively complex, and the treatment efficacy of TNBC is not satisfactory. The molecular mechanisms underlying the occurrence and development of TNBC need to be comprehensively interpreted. It has been shown that lncRNAs played important roles in BC progression.[20–26] More research has focused on the function and molecular mechanism of lncRNAs to find new targets for cancer diagnosis and therapy. In this article, we found that the expression of FOXCUT was significantly increased in TNBC tissues compared with that of normal tissues and that high expression of FOXCUT was related to poor prognosis in BC patients. Functional studies showed that FOXCUT could increase the proliferation and migration ability of TNBC cells *in vivo* or *in vitro*, suggesting FOXCUT had a cancer-promoting effect in TNBC. In this paper, through the sequencing of 196 BC tissues, the molecular mechanism of FOXCUT regulating TNBC progression by acting as a ceRNA was discovered.

The subcellular localization of lncRNAs determines their biological functions. Studies have revealed that lncRNAs localized in the cytoplasm can get involved in gene regulation at the posttranscriptional level, for example, they can inhibit the repression of target mRNAs by acting as ceRNAs.[27–31] Using RNA FISH and cytoplasmic/nuclear fractionation, we found that FOXCUT was preferentially located in the cytoplasm, suggesting that it had the potential to function as a miRNA sponge. Then, we found a binding site for miR-24-3p in the FOXCUT sequence by bioinformatic analysis, and this finding was further verified by luciferase reporter gene and RIP assays. Furthermore, FOXCUT was inversely correlated with the expression of miR-24-3p and repressed each other in BC cells. Importantly, miR-24-3p served as a tumor suppressor gene in BC, and overexpression of miR-24-3p partially reversed the FOXCUT-mediated promotion of BC cell proliferation, migration, and invasion. Fan *et al*[32] also suggested that FOXCUT might participate in angiogenesis and epithelial-mesenchymal transition by upregulating the expression levels of β-catenin and VEGF-A. Moreover, FOXCUT was correlated with the tumor progression of neck squamous cell carcinoma and basal-like BC by modulating its paired mRNA, FOXC1.[33,34] In addition, miR-24-3p was elucidated to negatively regulate ING1 expression to promote colon cancer carcinogenesis.[35] It

could also serve as a direct upstream repressor of CBS, which inhibited the development of hepatocellular carcinoma by suppressing the STAT3 pathway.[36] Taken together, our findings suggested that the lncRNA FOXCUT could act as a ceRNA by binding with miR-24-3p in BC.

However, the regulatory mechanisms of p38 expression and function in BC have not been fully elucidated. In this research, we identified p38 as a target gene of the FOXCUT/miR-24-3p axis based on the following observations. Bioinformatic analysis predicted that p38 was a direct target gene of miR-24-3p in BC cells, which was further confirmed by a dual-luciferase gene reporter assay. Moreover, overexpression of FOXCUT led to an increase in p38 expression, and this phenomenon could be partially reversed by overexpression of miR-24-3p, suggesting a FOXCUT/miR-24-3p/p38 axis in BC. We also discovered a significant positive correlation between the expression of FOXCUT and p38 in BC cells. In addition, we found that p38 was highly expressed in BC tissues, and knockdown of p38 could significantly inhibit the proliferation, migration, and invasion of BC cells. Significantly, downregulated p38 signaling has been demonstrated to be involved in DNA damage and chromosome instability, resulting in BC cell death.[37] Curtis *et al*[38] discovered that p38α MAPK activation facilitated the proliferation and metastasis of cancer cells by inducing glycogen mobilization. Furthermore, the disruption of p38 MAPK that was caused by extracellular vesicles released from pancreatic cancer cells could reduce the progression of pancreatic cancer.[39] Therefore, we further demonstrated the role of p38 as a BC proto-oncogene and provided data to support the molecular mechanism of p38 posttranscriptional regulation by lncRNAs in BC.

However, the present study leaves something to be desired, and it remains to be determined whether FOXCUT serves a cancer-promoting function other than as a microRNA sponge. In addition, the relatively small sample size may have limited the generalizability of these results as a biomarker for FOXCUT in the general population.

In conclusion, we identified the lncRNA FOXCUT as a proto-oncogene of TNBC, and high expression of FOXCUT was related to poor BC prognosis. FOXCUT acted as a sponge for miR-24-3p, attenuating its inhibitory effect on p38. Our study provided a novel understanding of the role of FOXCUT in BC progression and identified potential prognostic predictors and therapeutic targets for TNBC.

Funding

The current study was funded by the National Natural Science Foundation of China (Nos. 82072931 and 82002805).

Conflicts of interest

None.

References

1. Siegel RL, Miller KD, Wagle NS, Jemal A. Cancer statistics, 2023. CA Cancer J Clin 2023;73:17-48. doi:10.3322/caac.21763
2. Harbeck N, Penault-Llorca F, Cortes J, Gnant M, Houssami N, Poortmans P, *et al*. Breast cancer. Nat Rev Dis Primers 2019;5:66. doi: 10.1038/s41572-019-0111-2.
3. Sørlie T, Perou CM, Tibshirani R, Aas T, Geisler S, Johnsen H, *et al*. Gene expression patterns of breast carcinomas distinguish tumor subclasses with clinical implications. Proc Natl Acad Sci U S A 2001;98:10869–10874. doi: 10.1073/pnas.191367098.
4. Shah SP, Roth A, Goya R, Oloumi A, Ha G, Zhao Y, *et al*. The clonal and mutational evolution spectrum of primary triple-negative breast cancers. Nature 2012;486:395–399. doi: 10.1038/nature10933.
5. Bianchini G, De Angelis C, Licata L, Gianni L. Treatment landscape of triple-negative breast cancer-expanded options, evolving needs. Nat Rev Clin Oncol 2022;19:91–113. doi: 10.1038/s41571-021-00565-2.
6. Bianchini G, Balko JM, Mayer IA, Sanders ME, Gianni L. Triple-negative breast cancer: Challenges and opportunities of a heterogeneous disease. Nat Rev Clin Oncol 2016;13:674–690. doi: 10.1038/nrclinonc.2016.66.
7. Masuda H, Baggerly KA, Wang Y, Zhang Y, Gonzalez-Angulo AM, Meric-Bernstam F, *et al*. Differential response to neoadjuvant chemotherapy among 7 triple-negative breast cancer molecular subtypes. Clin Cancer Res 2013;19:5533–5540. doi: 10.1158/1078-0432.CCR-13-0799.
8. Yin L, Duan JJ, Bian XW, Yu SC. Triple-negative breast cancer molecular subtyping and treatment progress. Breast Cancer Res 2020;22:61. doi: 10.1186/s13058-020-01296-5.
9. Garrido-Castro AC, Lin NU, Polyak K. Insights into molecular classifications of triple-negative breast cancer: Improving patient selection for treatment. Cancer Discov 2019;9:176–198. doi: 10.1158/2159-8290.CD-18-1177.
10. Bartonicek N, Maag JL, Dinger ME. Long noncoding RNAs in cancer: Mechanisms of action and technological advancements. Mol Cancer 2016;15:43. doi: 10.1186/s12943-016-0530-6.
11. Lu TX, Rothenberg ME. MicroRNA. J Allergy Clin Immunol 2018;141:1202–1207. doi: 10.1016/j.jaci.2017.08.034.
12. Iorio MV, Croce CM. MicroRNA dysregulation in cancer: Diagnostics, monitoring and therapeutics. A comprehensive review. EMBO Mol Med 2012;4:143–159. doi: 10.1002/emmm.201100209.
13. Johnson JL. Elucidating the contributory role of microRNA to cardiovascular diseases (a review). Vascul Pharmacol 2019;114:31–48. doi: 10.1016/j.vph.2018.10.010.
14. Liang Y, Song X, Li Y, Chen B, Zhao W, Wang L, *et al*. LncRNA BCRT1 promotes breast cancer progression by targeting miR-1303/PTBP3 axis. Mol Cancer 2020;19:85. doi: 10.1186/s12943-020-01206-5.
15. Dykes IM, Emanueli C. Transcriptional and post-transcriptional gene regulation by long non-coding RNA. Genomics Proteomics Bioinformatics 2017;15:177–186. doi: 10.1016/j.gpb.2016.12.005.
16. Angrand PO, Vennin C, Le Bourhis X, Adriaenssens E. The role of long non-coding RNAs in genome formatting and expression. Front Genet 2015;6:165. doi: 10.3389/fgene.2015.00165.
17. Zhao DL, Shen G. Verification of expressions of lncRNA FOXCUT in gastric adenocarcinoma patients and its effects on cell biological function based on TCGA database. Eur Rev Med Pharmacol Sci 2019;23:6139–6147. doi: 10.26355/eurrev_201907_18427.
18. Zhang X, Yi S, Xing G, Wu H, Zhu Y, Guo X, *et al*. FOXCUT promotes the proliferation and invasion by activating FOXC1/PI3K/AKT pathway in colorectal cancer. Cancer Manag Res 2020;12:6269–6278. doi: 10.2147/CMAR.S259801.
19. Wang X, Hu Y, Cui J, Zhou Y, Chen L. Coordinated targeting of MMP-2/MMP-9 by miR-296-3p/FOXCUT exerts tumor-suppressing effects in choroidal malignant melanoma. Mol Cell Biochem 2018;445:25–33. doi: 10.1007/s11010-017-3248-x.
20. Wu XS, Wang F, Li HF, Hu YP, Jiang L, Zhang F, *et al*. LncRNA-PAGBC acts as a microRNA sponge and promotes gallbladder tumorigenesis. EMBO Rep 2017;18:1837–1853. doi: 10.15252/embr.201744147.
21. Matsumura K, Kawasaki Y, Miyamoto M, Kamoshida Y, Nakamura J, Negishi L, *et al*. The novel G-quadruplex-containing long non-coding RNA GSEC antagonizes DHX36 and modulates colon cancer cell migration. Oncogene 2017;36:1191–1199. doi: 10.1038/onc.2016.282.

22. Venkatesh J, Wasson MD, Brown JM, Fernando W, Marcato P. LncRNA-miRNA axes in breast cancer: Novel points of interaction for strategic attack. Cancer Lett 2021;509:81–88. doi: 10.1016/j.canlet.2021.04.002.
23. Wang YQ, Li HZ, Gong WW, Chen YY, Zhu C, Wang L, *et al*. Cancer incidence and mortality in Zhejiang province, Southeast China, 2016: A population-based study. Chin Med J 2021;134:1959–1966. doi: 10.1097/CM9.0000000000001666.
24. Cao W, Chen HD, Yu YW, Li N, Chen WQ. Changing profiles of cancer burden worldwide and in China: A secondary analysis of the global cancer statistics 2020. Chin Med J 2021;134:783–791. doi: 10.1097/CM9.0000000000001474.
25. Zheng A, Guo BL, Zhang JG, Jin F; Chinese Society of Breast Surgery. Clinical information and management status of de novo stage IV breast cancer patients: A Chinese multicenter investigation (CSBrS-002). Chin Med J 2021;134:1569–1575. doi: 10.1097/CM9.0000000000001415.
26. Jin YC, Du JX, Fu SM, Chen Q, Qiu YR, Pei A, *et al*. A retrospective clinical study of patients with pregnancy-associated breast cancer among multiple centers in China (CSBrS-008). Chin Med J 2021;134:2186–2195. doi: 10.1097/CM9.0000000000001697.
27. Cesana M, Cacchiarelli D, Legnini I, Santini T, Sthandier O, Chinappi M, *et al*. A long noncoding RNA controls muscle differentiation by functioning as a competing endogenous RNA. Cell 2011;147:358–369. doi: 10.1016/j.cell.2011.09.028.
28. Salmena L, Poliseno L, Tay Y, Kats L, Pandolfi PP. A ceRNA hypothesis: The Rosetta Stone of a hidden RNA language? Cell 2011;146:353–358. doi: 10.1016/j.cell.2011.07.014.
29. Xia C, Dong X, Li H, Cao M, Sun D, He S, *et al*. Cancer statistics in China and United States, 2022: Profiles, trends, and determinants. Chin Med J 2022;135:584–590. doi: 10.1097/CM9.0000000000002108.
30. Wang W, Wang X, Liu J, Zhu Q, Wang X, Wang P. Nomogram for predicting axillary lymph node pathological response in node-positive breast cancer patients after neoadjuvant chemotherapy. Chin Med J 2021;135:333–340. doi: 10.1097/CM9.0000000000001876.
31. Luo C, Li N, Lu B, Cai J, Lu M, Zhang Y, *et al*. Global and regional trends in incidence and mortality of female breast cancer and associated factors at national level in 2000 to 2019. Chin Med J 2021;135:42–51. doi: 10.1097/CM9.0000000000001814.
32. Fan CN, Ma L, Liu N. Comprehensive analysis of novel three-long noncoding RNA signatures as a diagnostic and prognostic biomarkers of human triple-negative breast cancer. J Cell Biochem 2019;120:3185–3196. doi: 10.1002/jcb.27584.
33. Hu Y, Guo G, Li J, Chen J, Tan P. Screening key lncRNAs with diagnostic and prognostic value for head and neck squamous cell carcinoma based on machine learning and mRNA-lncRNA co-expression network analysis. Cancer Biomark 2020;27:195–206. doi: 10.3233/CBM-190694.
34. Liu J, Shen L, Yao J, Li Y, Wang Y, Chen H, *et al*. Forkhead box C1 promoter upstream transcript, a novel long non-coding RNA, regulates proliferation and migration in basal-like breast cancer. Mol Med Rep 2015;11:3155–3159. doi: 10.3892/mmr.2014.3089.
35. Gao Z, Zhou L, Hua S, Wu H, Luo L, Li L, *et al*. miR-24-3p promotes colon cancer progression by targeting ING1. Signal Transduct Target Ther 2020;5:171. doi: 10.1038/s41392-020-0206-y.
36. Zhou YF, Song SS, Tian MX, Tang Z, Wang H, Fang Y, *et al*. Cystathionine beta-synthase mediated PRRX2/IL-6/STAT3 inactivation suppresses tregs infiltration and induces apoptosis to inhibit HCC carcinogenesis. J Immunother Cancer 2021;9:e003031. doi: 10.1136/jitc-2021-003031.
37. Cánovas B, Igea A, Sartori AA, Gomis RR, Paull TT, Isoda M, *et al*. Targeting p38alpha increases DNA damage, chromosome instability, and the anti-tumoral response to taxanes in breast cancer cells. Cancer Cell 2018;33:1094–1110.e8. doi: 10.1016/j.ccell.2018.04.010.
38. Curtis M, Kenny HA, Ashcroft B, Mukherjee A, Johnson A, Zhang Y, *et al*. Fibroblasts mobilize tumor cell glycogen to promote proliferation and metastasis. Cell Metab 2019;29:141–155.e9. doi: 10.1016/j.cmet.2018.08.007.
39. Yang J, Zhang Z, Zhang Y, Ni X, Zhang G, Cui X, *et al*. ZIP4 promotes muscle wasting and cachexia in mice with orthotopic pancreatic tumors by stimulating RAB27B-regulated release of extracellular vesicles from cancer cells. Gastroenterology 2019;156:722–734.e6. doi: 10.1053/j.gastro.2018.10.026.
40. Bian Q, Chen B, Weng B, Chu D, Tang X, Yan S, *et al*. circBTBD7 Promotes Immature Porcine Sertoli Cell Growth through Modulating miR-24-3p/MAPK7 Axis to Inactivate p38 MAPK Signaling Pathway. Int J Mol Sci 2021;22. doi: 10.3390/ijms22179385.
41. Sun L, Yao C, Li X, Wang Y, Wang R, Wang M, *et al*. Anastasis confers ovarian cancer cells increased malignancy through elevated p38 MAPK activation. Cell Death Differ 2023;30:809–824. doi: 10.1038/s41418-022-01081-1.

How to cite this article: Yu XF, Qian FZ, Zhang XQ, Zhu YH, He G, Yang JZ, Wu X, Zhou Y, Shen L, Shi XY, Zhang HF, Liu XA. Promotion effect of FOXCUT as a microRNA sponge for miR-24-3p on progression in triple-negative breast cancer through the p38 MAPK signaling pathway. Chin Med J 2024;137:105–114. doi: 10.1097/CM9.0000000000002700